Prepublished Copy

NATURE ENVIRONMENT AND POLLUTION TECHNOLOGY

Article In Press

PEER-REVIEWED PREPUBLISHED MANUSCRIPT

This is a peer-reviewed prepublished version of the paper to be published in **Vol. 26, No. 1, March 2027.**

Kinetics of Polylactic Acid Biodegradation Based on Multiparameter Carbon, Nitrogen and Moisture Dynamics in Windrow Composting Systems

Sujitha Ravi and Senthil Kumar. G.

RECEIVED
6 May 2026

CITE THIS ARTICLE
Sujitha Ravi and Senthil Kumar. G., 2027. Kinetics of Polylactic Acid Biodegradation Based on Multiparameter Carbon, Nitrogen and Moisture Dynamics in Windrow Composting Systems. Nature Environment and Pollution Technology, 26(1), B4451.

https://doi.org/10.46488/NEPT.2027.v26i01.B4451

EARLY-ACCESS STATEMENT

This manuscript, after peer review, is being released online in its original, unedited form to provide early access to its findings. Prior to final publication, it will undergo additional editing and formatting. Readers may note that, as an unedited version, the manuscript may have linguistic and other minor errors. The DOI will be active after the final publication of the paper.

PUBLICATION STATUS

PEER REVIEW	ONLINE VERSION	FINAL ISSUE
Completed	**Prepublished**	**March 2027**

Kinetics of Polylactic Acid Biodegradation Based on Multiparameter Carbon, Nitrogen and Moisture Dynamics in Windrow Composting Systems

Sujitha Ravi * and Senthil Kumar. G

Department of Civil Engineering, Annamalai University, Annamalainagar, Tamil Nadu, India

Corresponding author E-mail: sujitharavi215@gmail.com

Sujitha Ravi - 0009-0001-7763-1009

Senthil Kumar. G - 000-0003-4011-4726

Abstract

Polylactic acid (PLA) is a bioplastic of commercial significance. However, its degradation rate under practical conditions, such as windrow composting, has not been well established. This study attempted a detailed first-order kinetic study of the degradation of PLA-based biopolymers across six different heap setups over a 56-day composting period. Four interconnected parameters were examined: total organic carbon (TOC), volatile organic carbon (VOC), carbon-to-nitrogen (C/N) ratio, and gravimetric moisture content (MC). The raw data for these parameters were converted into normalized concentration ratios (Cs/C0) and their natural logarithms [ln (Cs/C0)] to enable linear regression analysis over the composting period (0–56 d, with samples taken every 7 d). The first-order rate constants (k) and coefficients of determination (R^2) were calculated for each heap parameter combination. The TOC degradation rate constants were found to be between 0.0135 and 0.0192 d^{-1}, with R^2 values ranging from 0.963 to 0.992. This indicates a strong adherence to first-order kinetics, consistent with substrate-limited degradation, although the relative contributions of microbial oxidation and abiotic hydrolysis were not independently quantified. The VOC rate constants ranged from 0.0105 to 0.0211 d^{-1}, with R^2 values between 0.913 and 0.991, highlighting the varying rates of volatilization and microbial oxidation among the compost heaps. The kinetics of the C/N ratio showed k values from 0.0092 to 0.0129 d^{-1} (R^2 = 0.81 to 0.96). This suggests that nitrogen immobilization and carbon depletion are kinetically linked but are influenced by the specific microbial communities in each heap. Moisture reduction followed a first-order decay pattern, with k values ranging from 0.0063 to 0.0130 d^{-1} and R^2 values ranging from 0.962 to 0.989 across all six heaps. The descriptors for empirical stabilization and attenuation concerning the C/N ratio and moisture content are expressed as first-order coefficients that differentiate them from the direct biodegradation rates. In contrast, the TOC and VOC constants genuinely reflect substrate-limited decays. Daily temperature observations showed a clear thermophilic phase, with temperatures between 53.4 and 59.4 °C, which is above the PLA glass-transition point. These temperatures remained at or above 45 °C for almost three weeks, providing the heat required for PLA ester bond hydrolysis. FTIR and SEM–EDS analyses provided clear molecular and structural evidence of PLA breakdown. By Day 56, the particles exhibited increasing surface erosion, cracking, and breaking apart. The FTIR spectra revealed methyl-ester and ester C–O–C bands alongside hydroxyl development, which aligned with ester bond hydrolysis. By Day 56, TOC reductions ranged from 64.9% to 71.6%, and the final C/N ratios were between 10.41 and 11.39, indicating significant physicochemical stabilization. This was further supported by a mildly alkaline pH (8.31–8.53), electrical conductivity below the 4.0 mS cm^{-1} phytotoxicity threshold, and near ambient final temperatures. These results establish first-order benchmarks for the composting behavior of PLA-amended windrows and provide direct FTIR and SEM evidence of PLA structural degradation under thermophilic conditions.

Keywords: Polylactic acid; first-order degradation kinetics; windrow composting; total organic carbon; C/N ratio; biopolymer solid waste management; volatile organic carbon

1. Introduction

The global prevalence of single-use plastics has triggered an environmental crisis of unprecedented scale, leading regulatory bodies and industries to seek viable bio-based alternatives (Geyer et al., 2017). Among commercially available bioplastics, polylactic acid (PLA) is the most extensively produced bio-derived thermoplastic, with a worldwide production capacity surpassing 400,000 tonnes annually and a projected compound annual growth rate of more than 10% until 2030 (European Bioplastics, 2023). Derived mainly from fermented plant materials such as maize starch and sugarcane, PLA possesses physical and mechanical properties similar to polystyrene and PET, making it a technically feasible substitute for food packaging, agricultural mulch films, and short-lifecycle consumer goods (Jem & Tan, 2020; Ncube et al., 2021).

Despite being sourced from bio-based materials, it does not break down under typical environmental conditions. The hydrolytic chain scission of its ester backbone, which limits the rate of PLA mineralization, occurs significantly only at temperatures above 55°C and in high-moisture environments, conditions found in thermophilic composting rather than in natural soil or marine environments (Rhim et al., 2013; Bagheri et al., 2017). This distinction is environmentally significant because PLA discarded in landfills, waterways, or open environments does not biodegrade within a meaningful timeframe (Piemonte et al., 2013). Consequently, managing PLA's end-of-life of PLA through certified industrial composting facilities is essential to realize its claimed environmental benefits (Hottle et al., 2017).

The composting of biopolymer waste involves a complex interplay of thermodynamic, microbiological, and physicochemical processes. From a kinetic perspective, the rates of organic carbon mineralization, volatile organic release, C/N ratio changes, and moisture reduction are critical in determining both the quality of compost and the economic feasibility of the process (Haug 1993; Komilis & Ham 2006). First-order kinetic models are often used in solid waste biodegradation studies. These models assume that the degradation rate at any time is proportional to the remaining substrate concentration. This assumption is well-supported for different organic materials when nutrients are not limited (Manna et al., 2017). Using the natural logarithm of the concentration ratio makes it easy to estimate rate constants (k) and check them statistically with the R^2 coefficient. No study has concurrently applied first-order kinetics to multiple degradation parameters, such as TOC, VOC, C/N, and moisture, across independently managed PLA-amended heaps, nor has it integrated these bulk kinetics with polymer-specific spectroscopic and morphological evidence. Existing research predominantly emphasizes weight loss or carbon dioxide evolution as the sole indicators of degradation (Nair et al., 2016; Ruggero et al., 2022), often neglecting the integration of multiple physicochemical parameters into a unified framework. Additionally, there is a lack of comparative multi-heap analyses that assess intra-experiment variability in rate constants and specifically investigate whether different heap formulations demonstrate statistically distinct degradation pathways. The concurrent parameterization of TOC mineralization, VOC dynamics, C/N evolution, and moisture loss within a uniform first-order framework for PLA composting systems remains unaccomplished.

The breakdown of biodegradable polymers in composting environments follows a structured sequence: initial abiotic hydrolysis of polymer chains, followed by enzymatic depolymerization through extracellular microbial enzymes, uptake of monomeric and oligomeric products by microbial communities, and finally, their conversion into carbon dioxide, water, and stable humic substances (Garlotta 2001; Rujnic-Sokele & Pilipović 2017). For PLA, the first and rate-determining step involves the hydrolysis of the ester bond between lactic acid monomers, which is enhanced by thermophilic temperatures (55–70°C), water activity, and the autocatalytic effect of the released carboxylic end groups (De Jong et al. 2001; Tsuji 2010).

Kale et al. (2007) showed that PLA films experienced over 90% mass loss within 30 d under controlled composting at 58°C, while no significant degradation occurred in soil burial tests during the same timeframe. Rudnik and Briassoulis (2011) verified that the degradation of injection-molded PLA items in municipal composting required prolonged thermophilic conditions and was influenced by the crystallinity of the feedstock, with amorphous PLA degrading much faster than semi-crystalline PLA degradation. Recently, Laycock et al. (2017) offered a comprehensive mechanistic model connecting the reduction in polymer molecular weight, as determined by gel permeation chromatography, to both temperature-dependent hydrolysis rate constants and the subsequent microbial assimilation of solubilized oligomers, outlining a two-phase kinetic model for PLA mineralization.

Consistent with this, home composting conditions (25–35°C) are insufficient to achieve appreciable PLA mass loss over extended periods, reinforcing the conclusion that industrial composting represents the only currently viable thermally driven end-of-life pathway (Kale et al. 2007; Rudnik and Briassoulis 2011; Ruggero et al. 2022). These findings are consistent with the position of international certification bodies, including EN 13432 and ASTM D6400, which mandate that certified compostable bioplastics achieve greater than 90% mineralization under thermophilic industrial composting conditions within 180 d (CEN 2000; ASTM 2019).

First-order kinetic models have a well-established theoretical basis in composting science, originating from the foundational work of Haug (1993), who described the consumption of biodegradable organic matter as a substrate-limited reaction with a rate that is proportional to the residual substrate mass.

The equation Ct = C0 · e-kt, where Ct represents the concentration of a parameter at time t, C0 is the starting concentration, and k is the first-order rate constant (day-1), has been extensively validated using experimental data from composting municipal solid waste, food waste, and lignocellulosic materials (Komilis & Ham 2006, Manna et al. 2017). By applying a natural logarithm transformation, the equation becomes ln(Ct/C0) = −kt, allowing for the graphical determination of k from the linear regression slope and evaluation of the model accuracy using the coefficient of determination (R^2).

In their study, Manna et al. (2017) utilized first-order kinetics to examine organic carbon degradation in municipal solid waste composting with five different feedstock combinations, finding k values between 0.008 and 0.024 day^{-1}, with R^2 values consistently above 0.94. Similarly, the dynamics of the C/N ratio have been observed to exhibit first-order behavior during the active thermophilic phase in other composting systems (Manna et al. 2017; Ruggero et al. 2022). Ruggero et al. (2022) applied first-order kinetics to the degradation of rigid and film bioplastics, including PLA, under less-than-ideal composting conditions, showing that first-order models effectively described the reduction of carbon-related parameters, with rate constants influenced by the aeration rate and initial C/N ratio. However, a simultaneous first-order kinetic analysis of the TOC, VOC, C/N ratio, and moisture content of PLA biopolymers across various independently managed heap configurations has not been documented. This study addresses this gap by providing a comprehensive multiparameter, multi-heap kinetic dataset for PLA-based composting systems.

The C/N ratio is vital factor in the composting process that indicating the equilibrium between carbon breakdown and nitrogen retention. An initial C/N ratio of 25–30 is typically considered ideal for facilitating thermophilic microbial activity (Haug 1993; Bernal et al. 2009). During composting, carbon is lost more rapidly through CO^2 release than nitrogen through volatilization, provided that the process is well managed, leading to a gradual decrease in the C/N ratio. Mature and stable compost is usually identified by a C/N ratio below 15–20, with values under 12 signifying high maturity (Lazcano et al. 2008; Bernal et al. 2009). The rate at which the C/N ratio decreases has been suggested as an indicator of maturity and is linked to both temperature changes and the turnover of microbial biomass (Tiquia et al. 1996).

Moisture content serves as both a substrate for microbial activity and a byproduct of the metabolic oxidation of organic matter. The ideal moisture content for composting is between 50% and 65% (based on wet weight), as levels below this limit lead to insufficient water for microbial metabolism, while levels above can lead to anaerobic conditions (Agnew & Leonard 2003). The decline in moisture content during composting is due to evaporative losses driven by the thermophilic heat gradient, consumption of water through metabolism, and aeration from turning. Measuring the kinetics of moisture reduction helps predict the duration of active microbial decomposition and the beginning of the maturation phase (Hamelers 2004).

This study addresses these shortcomings by implementing an extensive first-order kinetic analysis on six separately managed windrow heaps, monitoring four degradation parameters weekly over a period of 56 days. The specific aims were as follows: (i) to determine first-order rate constants for TOC, VOC, C/N ratio, and moisture content across all heap setups; (ii) to evaluate the first-order model's fit using R^2 analysis; (iii) to detect and explain variations in kinetic parameters between heaps in relation to established composting microbiology; and (iv) to assess the level of compost maturity reached at the end of the process against recognized quality standards. The findings of this study aim to offer quantitative kinetic benchmarks that are useful for industrial biopolymer waste management, biodegradable polymer certification systems, and the development of predictive composting process models.

2. Materials and Methods

2.1 Biopolymer Feedstock and Heap Configuration

The biopolymer substrate used was a post-consumer polylactic acid (PLA) packaging film. This film is certified as compostable under IS/ISO 17088 standards by the Central Pollution Control Board (Government of India) and is described by the supplier as a PLA/PBAT formulation. The film was mechanically shredded, without chemical pre-treatment, into particles smaller than 2 mm to increase the surface area available for microbial colonization and to represent realistic post-consumer disposal conditions. The common composting matrix for all heaps comprised fresh vegetable waste (VW) as the primary putrescible substrate and cow dung (CD) as the microbial inoculum and activator, supplying an indigenous consortium of cellulolytic and proteolytic microorganisms.

Six windrow heaps (Heaps 1–6) were operated simultaneously on a common VW + CD base and differed in a single controlled variable: PLA loading. Heap 1 was the unamended control (VW + CD, 0% PLA), and heaps 2–6 received PLA at 10, 20, 30, 40, and 50% by weight of the total composting substrate, respectively. No invasive green-biomass amendment, supplementary bulking agent, or variation in inoculum loading was applied; the vegetable waste-to-cow dung base and cow dung inoculum were held constant across all heaps so that any difference in composting behavior could be attributed to the PLA loading alone. Each heap was constructed to standardized trapezoidal dimensions of 2.0 m (length) × 1.5 m (breadth) × 1.2 m (height) on a level impermeable concrete base, turned manually at 7-day intervals to maintain aerobic conditions, and monitored to maintain moisture within the operational range of 50–60% by means of controlled sprinkler supplementation. All treatments were prepared and analyzed in triplicate. The composition and measured Day 0 characteristics of the six heaps are summarized in Table 1, and the physicochemical properties of the VW and CD feedstocks are listed in Table 2.

At the point of assembly (Day 0), the six heaps presented a consistent baseline, modulated by PLA loading. The initial pile temperatures ranged from 31.5 °C (Heap 6, 50% PLA) to 35.1 °C (Heap 1, control), close to the ambient temperature of 29.9 °C, confirming that exothermic microbial activity had not yet begun. The initial pH was slightly acidic to near-neutral (6.51 in Heap 1 to 6.82 in Heap 6), and the initial moisture ranged from 60.22 to 67.12%, within or marginally above the 50–65% operational optimum; both pH and moisture showed a weak inverse relationship with PLA loading, reflecting the dilution of the moisture-rich VW and CD fractions by the drier polymer.

Table 1. Configuration and initial (Day 0) characteristics of the six PLA composting heaps.							
Heap	**Treatment**	**PLA (% w/w)**	**Base VW+CD (% w/w)**	**Green-biomass amendment**	**Inoculum**	**Initial moisture (%)**	**Initial C/N**
1	VW+CD (control)	0	100	None	Cow dung*	62.00	27.53
2	VW+CD + 10% PLA	10	90	None	Cow dung*	65.46	29.22
3	VW+CD + 20% PLA	20	80	None	Cow dung*	65.10	27.96
4	VW+CD + 30% PLA	30	70	None	Cow dung*	67.12	25.17
5	VW+CD + 40% PLA	40	60	None	Cow dung*	65.12	27.16
6	VW+CD + 50% PLA	50	50	None	Cow dung*	60.22	25.18

Table 2. Initial physicochemical characteristics of the vegetable waste and cow dung feedstocks.		
Parameter	**Vegetable waste (VW)**	**Cow dung (CD)**
pH	7.9	7.8
Electrical conductivity (mS cm^{-1})	1.25	1.54
Moisture (%)	56	62
Total organic carbon, TOC (%)	43.5	36.54
Total Kjeldahl nitrogen, TKN (%)	1.98	1.75
C/N ratio	21.96	20.88
Volatile organic carbon, VOC (%)	75	63
Ash content (%)	55	48

The initial total organic carbon and volatile organic carbon were 36.39–53.06% and 62.50–73.30%, respectively, consistent with the high volatile content of fresh vegetable waste, while the initial C/N ratios of 25.17–29.22 reflected the combined stoichiometry of VW (C/N 21.96), CD (C/N 20.88), and the nitrogen-free PLA fraction, which increased the mixture C/N in proportion to loading. These baseline values confirmed that all heaps began within the recommended ranges for thermophilic composting and differed systematically only in the degree of PLA incorporation.

2.2 Sampling Protocol and Analytical Methods

The analysis took place in the Environmental Engineering and Analytical Chemistry Laboratory at Annamalai University. The analyses were conducted in accordance with ISO, IS, ASTM, and APHA standards. Before testing, composite samples were air-dried, oven-dried, ground, and sieved to obtain particles smaller than 2 mm. Instruments were calibrated with certified standards before each test session. For each series of tests, reagent blanks, matrix spikes, and triplicate measurements were incorporated. The findings are expressed as the mean ± standard deviation, calculated on a dry weight basis. Representative composite samples were collected from each heap at 7-day intervals on days 0, 7, 14, 21, 28, 35, 42, 49, and 56. Sampling was performed using a stratified

random protocol across five spatial locations within each heap cross-section to minimize spatial heterogeneity. All analyses were performed in triplicate, and arithmetic means were reported.

Total organic carbon (TOC) was determined using the modified Walkley-Black wet-oxidation method (Walkley and Black 1934; Nelson and Sommers 1982). A 0.500 ± 0.001 g portion of oven-dried, ground compost was oxidized with 10.0 mL of 1.0 N potassium dichromate and 20 mL of concentrated sulfuric acid, and the exothermic reaction reached approximately 120 °C. After 30 min, the excess dichromate was back-titrated against standardized 0.5 N ferrous ammonium sulfate using a diphenylamine indicator with a simultaneous reagent blank. A correction factor of 1.334 was applied to the mean oxidation-recovery efficiency of the method. To confirm analytical validity, TOC values were cross-checked against total carbon measured by dry combustion on a LECO CN-828 analyzer for a 10% subset of samples, with agreement within ± 8%. This wet-oxidation procedure directly measures oxidizable organic carbon and was used in preference to loss-on-ignition, which quantifies only bulk volatile matter and is not equivalent to a direct organic-carbon determination.

In this study, volatile organic carbon (VOC) denotes the volatile (combustible) organic fraction of the compost expressed as a percentage of dry mass and not speciated volatile organic compounds. It was determined gravimetrically by loss on ignition: 3.000 ± 0.001 g of oven-dried sample was ignited in a programmable muffle furnace ramped to 550 ± 10 °C at 100 °C h^{-1} and held for 4 h until a constant grey-white ash residue was obtained, then cooled in a desiccator, and re-weighed to constant mass. The ash content was calculated as the residual mass fraction, and the volatile organic fraction as VOC (%) = 100 − ash (%). Therefore, the parameter represents the proportion of oxidizable organic matter in compost. It was not measured by gas chromatography and did not involve target compound calibration; therefore, its progressive decline reflected the mineralization of organic matter to CO_2 and the relative accumulation of the inorganic ash fraction. For clarity, the term VOC is retained throughout, but it is equivalent to the volatile solids (volatile organic matter) fraction.

The C/N ratio was calculated from the total Kjeldahl nitrogen (TKN) determined by semi-micro Kjeldahl digestion and distillation (APHA 2017) and total organic carbon (TOC). Moisture content was determined gravimetrically by oven-drying at 105°C to a constant mass (ISO 11465, 1993). Heap temperature was recorded daily throughout the 56-day trial using a digital compost probe (Hanna HI9813-5) inserted at three depths (top, middle, and bottom) of each heap, and the heap mean was logged. The ambient temperature during the trial averaged 29.9 °C. The temperatures corresponding to the 7-day sampling schedule are listed in Table 3. All determinations were performed in triplicate, and the mean coefficient of variation among replicates was below 9%, confirming good analytical reproducibility. This is because the replicate scatter was small relative to the temporal trend. The mean values are plotted for clarity, and the uncertainty in the derived kinetics is expressed through the 95% confidence intervals of the rate constants.

2.3 First-Order Kinetic Modeling

First-order degradation kinetics were applied independently to each parameter-heap combination. The model assumes that the rate of change of the parameter concentration (C) with respect to time (t) is proportional to the current concentration:

$$dC/dt = -kC, \ldots\ldots\ldots\ldots (1)$$

where k is the first-order rate constant (day^{-1}).

Integration yields the exponential decay function

$$Ct = C0 \cdot e - kt, \ldots\ldots\ldots\ldots (2)$$

which upon linearization gives

$$ln(Ct/C0) = -kt. \ldots\ldots\ldots\ldots (3)$$

For each parameter, the normalized concentration ratio (Cs/C0) was computed at each time point, where Cs is the measured value and C0 is the initial value on day 0. The natural logarithm of this ratio [ln(Cs/C0)] was plotted against time in days and subjected to ordinary least-squares linear regression. The negative of the regression slope yields k, and the coefficient of determination (R^2) quantifies the model fit.

The four parameters modelled here fall into two mechanistically distinct classes, and the first-order framework is applied to them with different interpretations. Total organic carbon and volatile organic carbon are direct measures of the biodegradable substrate pool; for these, the first-order model represents genuine substrate-limited biodegradation, in which the oxidation rate is proportional to the residual carbon concentration. In contrast, the carbon-to-nitrogen ratio and moisture content are not primary substrate pools. The C/N ratio is a derived quantity, C/N = TOC / TKN, whose logarithmic form ln(C/N) = ln(TOC) − ln(TKN) shows that its decline is the compound result of first-order carbon loss superimposed on a progressive rise in nitrogen concentration, rather than a single decay process. Moisture loss is governed by evaporation, turning-induced aeration, and metabolic heat generation rather than biodegradation. For these two parameters, the first-order coefficient is therefore reported and interpreted as an empirical descriptor of the temporal trajectory, namely a C/N stabilization coefficient and a moisture attenuation coefficient, and not as a direct biodegradation rate constant. Their inclusion is justified on the grounds that both trajectories are paced by the underlying first-order carbon mineralization: the C/N ratio because its numerator decays first-order, and the moisture content because evaporative loss is proportional to the metabolic heat released during substrate oxidation (Haug, 1993; Hamelers, 2004). This coupling produces the approximately log-linear behavior observed, while the weaker and more variable fit obtained for the C/N ratio relative to TOC is a direct consequence of its compound-derived ratio nature.

All statistical analyses were performed in Microsoft Excel (Version 2021) with regression validated using Python SciPy (v1.9.3). An R^2 threshold of 0.80 was adopted as the minimum criterion for the acceptance of the first-order model.

The uncertainty in each first-order rate constant was quantified as the standard error of the regression slope, from which 95% confidence intervals were derived using the t-distribution (n = 9, df = 8). All physicochemical determinations were performed in triplicate and are reported as the mean ± standard deviation on a dry-weight basis.

2.4 Compost Maturity Assessment

Terminal compost maturity was evaluated against multiple criteria: (i) final C/N ratio below 15 (Bernal et al. 2009); (ii) TOC reduction greater than 50% (Haug 1993); (iii) terminal pH within 7.5–8.5 and (iv) electrical conductivity below 4.0 mS cm^{-1} (European Commission 2001); and (v) return of heap temperature to near-ambient values, indicating thermal stabilisation. These criteria were applied to the Day 56 data for all six heaps. Biological maturity indicators, namely the germination index, respiration rate and phytotoxicity bioassay, were not determined in this study and are recommended for future work.

3. Results and Discussion

3.1 Temperature Evolution and Thermophilic Dynamics

All six heaps followed the classic windrow thermal trajectory (Table 3). Initial temperatures were close to the ambient value of 29.9 °C (31.5–35.1 °C), confirming that exothermic activity had not yet begun. Within 24–48 h a strong exothermic transition raised every heap into the thermophilic range, with peak temperatures of 53.4–59.4 °C recorded during the initial burst. Weekly sampled temperatures remained thermophilic (≥ 45 °C) through

approximately Day 21 (51.3–54.6 °C at Day 7, 47.6–50.4 °C at Day 14 and 40.6–47.8 °C at Day 21), then declined through the mesophilic and maturation phases to 30.2–31.5 °C by Day 56, confirming thermal stabilization and the cessation of net exothermic activity. Thermogenic intensity varied systematically with PLA loading. Because PLA is thermally inert and supplies no readily fermentable carbon, increasing its proportion diluted the exothermic VW + CD substrate pool and lowered both the initial and the sustained temperatures, an effect most evident in the 40 and 50% PLA heaps (Heaps 5 and 6), which cooled most rapidly after Day 21. The intermediate 20% PLA heap (Heap 3) nevertheless achieved the highest peak temperature (59.4 °C), indicating a priming interaction in which limited abiotic hydrolysis of PLA ester bonds during the initial high-temperature window releases bioavailable lactic acid that supplements the declining vegetable-waste carbon pool and briefly sustains exothermy beyond the VW + CD baseline. These temperature data are mechanistically central to the degradation evidence reported in Section 3.6 of this study. PLA hydrolysis is strongly temperature-dependent and becomes appreciable only above the polymer glass-transition temperature (Tg ≈ 55–60 °C), at which the amorphous chain segments become mobile and ester bonds are accessible to water and microbial esterases (Tokiwa and Calabia 2006; Kale et al. 2007). The peak temperatures of 53–59 °C attained during the early thermophilic phase provided the thermal window required to initiate abiotic ester-bond hydrolysis, generating the carboxyl- and hydroxyl-terminated chain ends detected by FTIR and the progressive surface erosion documented by SEM. This confirms that the PLA degradation observed here proceeded under genuinely thermophilic conditions and is therefore directly relevant to industrial composting practice. The thermal regime also underlies the kinetic differences among heaps. The highest first-order TOC degradation rate constants were obtained in Heaps 3 and 4 ($k = 0.0192$ and $0.0184\ d^{-1}$, respectively), which combined intense early thermophilicity with sufficient labile substrate, whereas the 40% PLA heap (Heap 5) recorded both attenuated sustained temperatures and the lowest TOC rate constant ($k = 0.0135\ d^{-1}$). Because metabolic heat production is proportional to the substrate oxidation rate, the same thermophilic intensity that accelerated carbon mineralisation also drove evaporative moisture loss: Heap 3, with the highest peak temperature, showed the greatest moisture reduction (65.10 to 29.50%). The temperature profiles thus provide a coherent thermal explanation for the inter-heap variation in the TOC, VOC and moisture rate constants, linking the thermophilic phase directly to both the degradation kinetics and the polymer-level breakdown of PLA.

Table 3. Heap temperature (°C) at 7-day intervals during 56-day windrow composting for the six PLA loadings.

Day	Heap 1 (0%)	Heap 2 (10%)	Heap 3 (20%)	Heap 4 (30%)	Heap 5 (40%)	Heap 6 (50%)
0	35.1	33.2	34.6	34.6	32.4	31.5
7	52.4	54.1	51.3	52.3	51.4	54.6
14	47.6	49.7	48.7	48.4	50.4	49.8
21	40.6	45.8	44.6	45.5	47.8	43.2
28	34.2	32.1	32.4	34.5	42.2	40.6
35	33.5	34.6	35.4	32.7	36.7	32.9
42	32.1	38.6	34.6	33.5	31.5	31.5
49	32.1	32.1	32.1	31.8	30.8	28.5
56	30.2	30.6	30.2	30.6	31.5	30.3

3.2 Total Organic Carbon

Table 1 and Figure 1 illustrate the changes in TOC over time for all six heaps. On Day 0, the initial TOC values varied between 36.39 g kg^{-1} dry weight in Heap 5 and 53.06 g kg^{-1} in Heap 2, indicating variations in the initial PLA loading and the composition of the bulking agents used in different heap setups. By Day 56, TOC levels had decreased to between 12.06 and 17.99 g kg^{-1}, marking a reduction of 60.9 to 71.6% across the heaps. This significant decrease aligns with the active thermophilic mineralization of the PLA carbon fraction and matches the TOC reduction range observed in other bioplastic composting systems (Ruggero et al. 2022) and in mixed organic waste composting, as reported by Komilis & Ham (2006), who showed reductions of 55–68% over 42 d.

During the composting process, the normalized total organic carbon (TOC) ratio (Cs/C0) in all heaps exhibited a consistent decline from an initial value of one on Day 0. By Day 56, this ratio reached a minimum of 0.284 in Heap 3 and a maximum of 0.491 in Heap 5. The ln(Cs/C0) profiles demonstrated a strong linear correlation with composting duration across all heaps, indicating first-order kinetics. The rate constants for TOC degradation, which followed first-order kinetics, varied from k = 0.0135 d^{-1} in Heap 5 to k = 0.0192 d^{-1} in Heap 3, with R^2 values ranging from 0.963 to 0.992. Notably, Heap 3 exhibited the highest TOC rate constant (k = 0.0192 d^{-1}), corresponding with a higher initial nitrogen content. This observation aligns with the hypothesis that nitrogen availability enhances microbial carbon oxidation, although microbial community composition and activity were not directly assessed in this study (Tiquia et al. 1996; Bernal et al. 2009).

The lower TOC rate constant in Heap 5 (k = 0.0135 d^{-1}) may be attributable to the relatively low initial TOC (36.39 g kg^{-1}) in this heap, which reduces the substrate gradient that drives the microbial mineralization. Furthermore, the terminal TOC value of 17.88 g kg^{-1} in Heap 5 on Day 56 represented only a 50.9% reduction, the lowest among all heaps, suggesting that either the composting period was insufficient or that a greater fraction of recalcitrant carbon was present in the initial material. This kinetic behavior is consistent with the substrate depletion effects described by Hamelers (2004), in which the effective rate constant decreases as easily degradable fractions are consumed and more refractory carbon is accumulated. The strong R^2 values across heaps (mean R^2 = 0.979) confirmed that first-order kinetics adequately described TOC mineralization in PLA-based composting systems, supporting the application of this model for process prediction and design.

Throughout the following analysis, the PLA-amended heaps (Heaps 2–6) are interpreted relative to the 0% PLA control (Heap 1), so that the influence of PLA loading is assessed against a constant vegetable-waste, cow-dung and inoculum background.

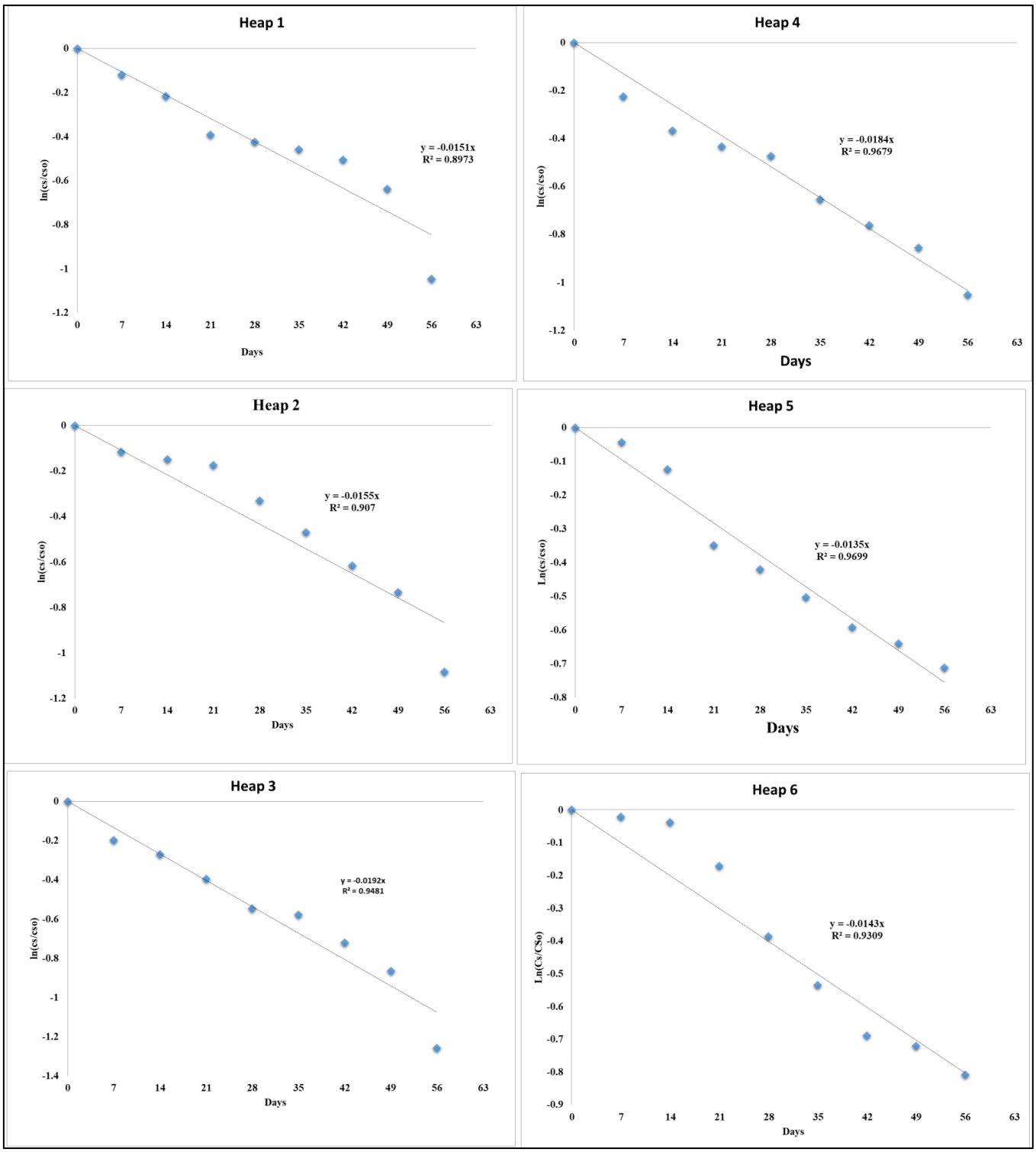

Figure 1: ln(TOC/TOC$_0$) versus composting time (days 0 to 56) for Heaps 1 to 6. Linear regression lines with R^2 values displayed for each heap. X-axis: Time (days); Y-axis: ln(Cs/C$_0$).

3.3 Volatile Organic Carbon Degradation Kinetics

VOC dynamics (Table 2, Figure 2) exhibited a pattern largely akin to TOC, though with distinct variations specific to each heap. Initially, VOC values on a dry weight basis ranged from 62.50% in Heap 1 to 73.30% in Heap 3, indicating the percentage of easily volatilizable carbonaceous components in the starting PLA biopolymer material. During the early stage (days 0–21), the reduction in VOC was significantly slower in Heaps 3 and 4 than in Heaps 1 and 2. This suggests that the higher nitrogen amendment in Heaps 3 and 4 might have initially shifted microbial processes towards protein breakdown and nitrogen cycling, rather than the oxidation of volatile carbon.

The first-order rate constants for VOC ranged from $k = 0.0105\ d^{-1}$ in Heap 6 to $k = 0.0211\ d^{-1}$ in Heap 1, with R^2 values between 0.913 and 0.991, as shown in Table 5. Heap 1 had the highest VOC rate constant that matched with its low initial C/N ratio, likely supporting a microbial community that quickly used volatile carbon. Heap 4 had the lowest R^2 value of 0.913 because VOC levels stayed almost the same from Days 7 to 28. During this time, Cs/C0 decreased from 0.99 to 0.82 over 21 days before dropping more quickly. This two-phase pattern can be explained by an initial lag phase where PLA hydrolysis products build up until microbial communities that can break down PLA oligomers grow enough, as noted by Laycock et al. (2017) in their study on PLA mineralization kinetics.By Day 56, terminal VOC values ranged from 24.03% in Heap 2 to 34.28% in Heap 6 on a dry weight basis, indicating reductions of 50.5 to 71.1% from initial values. Heap 6 experienced the smallest absolute reduction in VOC, with its k value of $0.0105\ day^{-1}$ being the lowest among all heaps. This slower VOC kinetics in Heap 6 might be due to a higher proportion of slowly hydrolyzable semi-crystalline PLA fractions in its feedstock (Tsuji 2010), or suboptimal thermophilic temperature maintenance caused by its modified bulking agent composition, affecting heap insulation. The VOC rate constants found in this study ($0.0105–0.0211\ d^{-1}$) align with those reported by Manna et al. (2017) for volatile solids in municipal solid waste composting ($0.00–0.024\ d^{-1}$), providing cross-validation for the first-order kinetics approach.

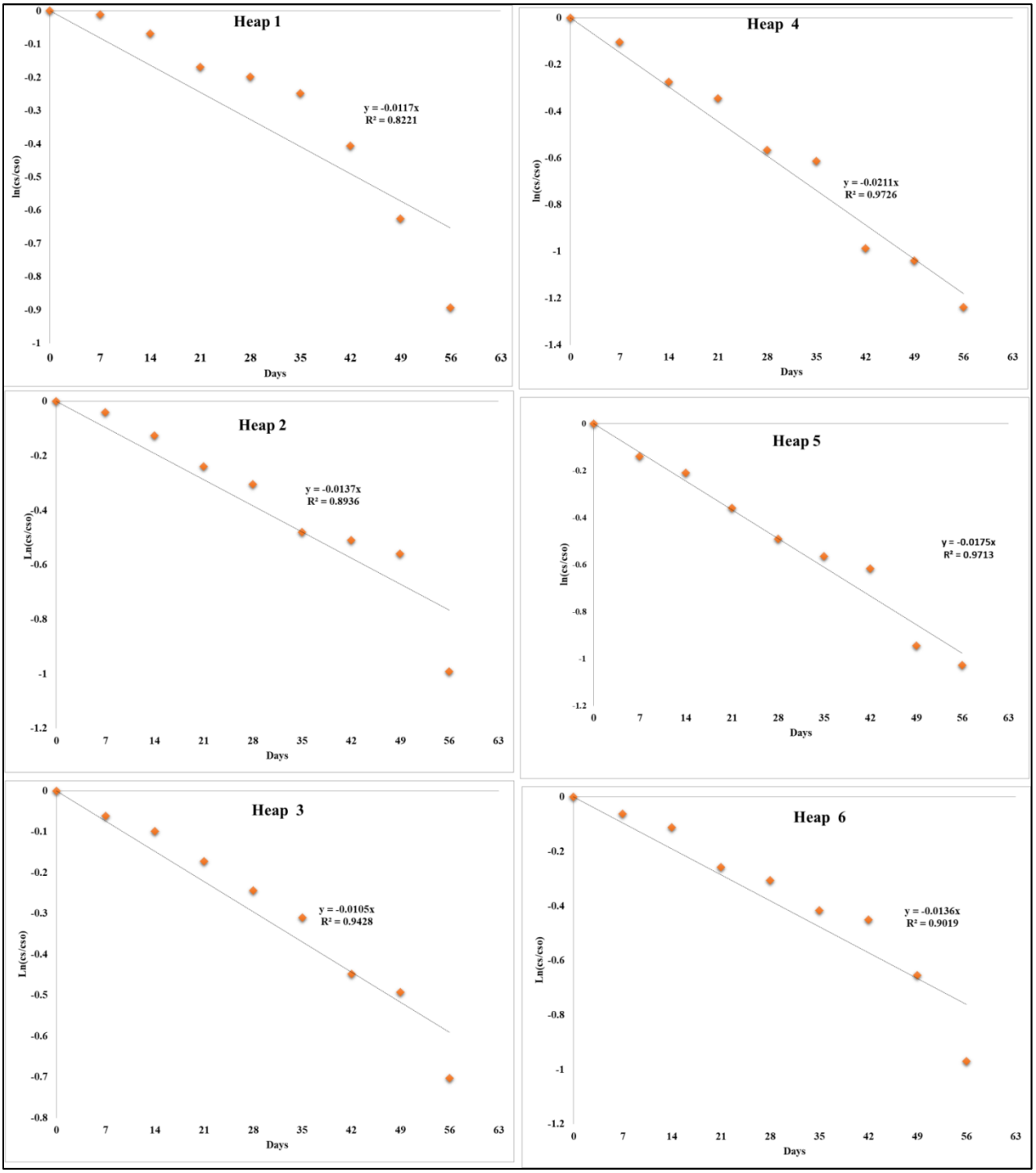

Figure 2: ln(VOC/VOC$_0$) versus composting time (days 0 to 56) for Heaps 1 to 6

3.4 Carbon-to-Nitrogen Ratio Dynamics

The C/N ratio is one of the most diagnostically informative composting parameters, integrating both carbon depletion and nitrogen conservation into a single index of microbial process efficiency (Bernal et al. 2009). Initial C/N ratios ranged from 25.17 (Heap 4) to 29.22 (Heap 2), all within the conventionally recommended range of 25 to 30 for optimal thermophilic composting (Haug, 1993). The progressive decline in C/N across all heaps (Table 3, Figure 3) reflects the preferential loss of carbon through CO^2 evolution and volatile organic release relative to nitrogen, which is partially conserved through immobilization into the microbial biomass. By Day 56, all heaps achieved terminal C/N ratios of 10.41 (Heap 4) to 11.39 (Heap 2), which were well below the threshold of 15 conventionally used to define compost maturity (Bernal et al. 2009). This represents an absolute decline of 58.7–64.3% relative to the initial values, confirming the advanced stabilization of the organic fraction. The first-order rate constants for C/N dynamics ranged from $k = 0.0092\ d^{-1}$ (Heap 4) to $k = 0.0129\ d^{-1}$ (Heap 3), with R^2 values of 0.807 to 0.962 across all six heaps. The convergence of terminal C/N values across all heaps (10.41 to 11.39) despite differing initial conditions and rate constants is a notable finding, suggesting that the composting system approaches a common thermodynamic endpoint dictated by the chemical composition of the PLA substrate and available nitrogen pool rather than pathway kinetics. On recalculation and verification, the first-order fit for the Heap 2 C/N ratio yielded $k = 0.0119\ day^{-1}$ with $R^2 = 0.82$, in agreement with the regression shown in Figure 3. The value of $R^2 = 0.092$ reported previously was a transcription error and has been corrected; Heap 2 is therefore not anomalous, but rather one of the better-fitting C/N series. All six heaps consequently conformed to the first-order stabilisation trend within the expected range, the C/N ratio showing the lowest and most variable goodness-of-fit of the four parameters for the derived-ratio reasons set out in Section 2.3. It is emphasised that the C/N ratio is a derived index rather than a directly degraded substrate, and its first-order coefficient is interpreted here as an empirical stabilisation rate rather than a degradation rate. The observed decline reflected two superimposed processes: the first-order loss of organic carbon and a concurrent rise in total Kjeldahl nitrogen, which increased over the trial, for example from 1.24 to 1.92% in the control heap and from 1.15 to 1.99% in the 20% PLA heap, as carbon was mineralised and nitrogen was concentrated and microbially immobilised. Consistent with this compound origin, the C/N ratio showed the lowest and most variable goodness-of-fit of the four parameters, and the C/N stab[illegible] r[illegible] spe[illegible] 9[illegible]

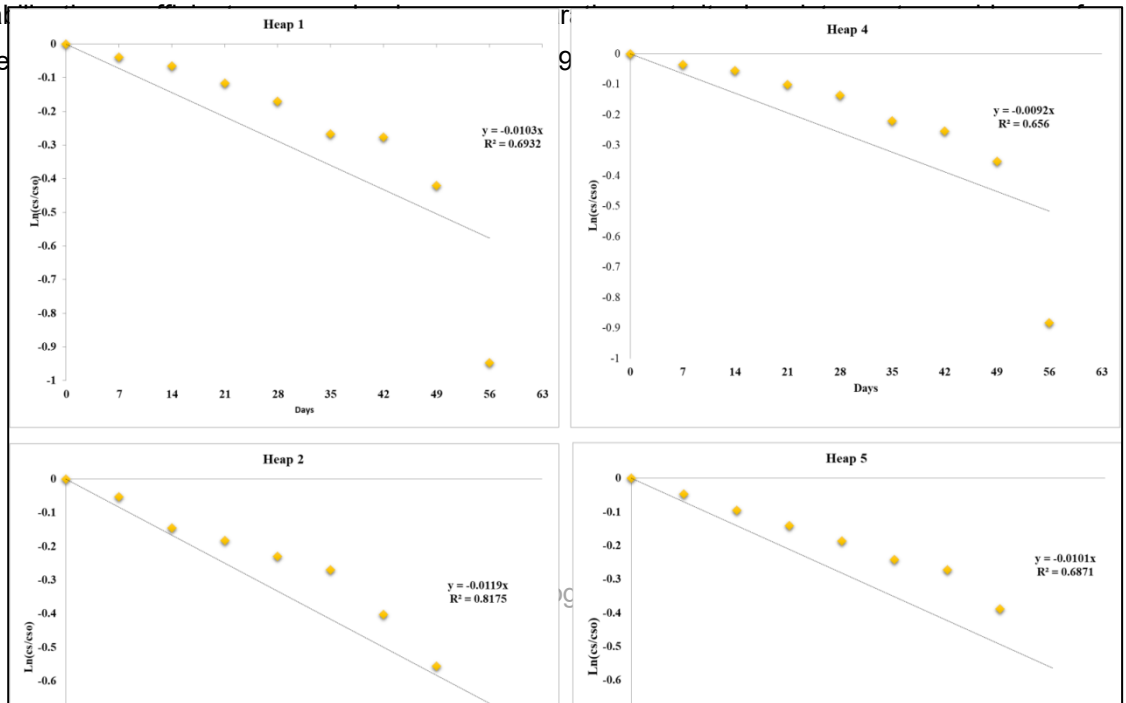

Figure 3: ln(C/N / C/N_0) versus composting time for Heaps 1 to 6. The anomalous Heap 2 trajectory should be visually evident and annotated. X-axis: Time (days); Y-axis: ln(Cs/C_0). Include dashed regression lines for all heaps.

3.5 Moisture Content

Moisture content is a prerequisite for microbial activity and a consequence of metabolic heat generation and evaporative losses during thermophilic composting (Agnew & Leonard 2003). The initial moisture content across the six heaps ranged from 60.22 (Heap 6) to 67.12% (Heap 4), all within the optimal range for thermophilic composting (Hamelers, 2004). Progressive moisture loss was observed in all heaps through the 56-day period (Table 4, Figure 4), with terminal values of 29.50% (Heap 3) to 40.45% (Heap 6). The wide range of terminal moisture values reflects the differences in heap geometry, turning frequency effects, and varying proportions of bulking agents with different water-holding capacities.

First-order rate constants for moisture attenuation ranged from k = 0.0063 day^{-1} (Heap 6) to k = 0.0130 day^{-1} (Heap 3), with R^2 values of 0.962 to 0.989 across all six heaps. The first-order moisture attenuation coefficient for Heap 5 was k = 0.0095 day^{-1} (R^2 = 0.96), consistent with Figure 4 and lying within the coherent range of 0.0063 to 0.0130 day^{-1} observed across the heaps. The previously tabulated value of 0.0995 day^{-1} was a transcription error and has been corrected. With this correction, moisture attenuation was well described by the empirical first-order model in all six heaps, and no value requires exclusion from the analysis. The moisture attenuation rate constants observed here display a coherent range consistent with rates reported by Hamelers (2004) for windrow composting systems (0.006 to 0.015 day^{-1}).

The faster moisture attenuation in Heap 3 (k = 0.0130 day^{-1}) is consistent with its greater overall organic matter degradation rate, as metabolic heat production is proportional to substrate oxidation rate and drives evaporative moisture loss (Haug 1993). Heap 6, with the lowest moisture rate constant (k = 0.0063 day^{-1}), also exhibited the highest terminal moisture content (40.45%), indicating that this

heap maintained higher water activity throughout the composting period. While this would theoretically support continued microbial activity, the terminal C/N ratio (11.16) and TOC reduction (55.5%) in Heap 6 suggest that degradation was not disproportionately advanced, implying that moisture alone was not the rate-limiting factor in slower-degrading heaps. The consolidated first-order rate constants and R^2 values for all parameter-heap combinations are presented in Table 5. The data collectively demonstrate that first-order kinetics provide an adequate to excellent description of PLA biopolymer degradation across the parameters measured, with the C/N ratio and moisture content interpreted as empirical stabilisation and attenuation descriptors (Section 2.3).

Across the four parameters, TOC degradation exhibited the highest overall goodness-of-fit, followed by moisture content and VOC, with the C/N ratio the lowest and most variable, all computed over the full set of six heaps without exclusions. The superior model fit for TOC is attributable to the inherent smoothness of bulk carbon mineralisation, which integrates across a heterogeneous microbial community and is therefore less susceptible to localised process perturbations than individual carbon fraction metrics such as VOC. The comparatively lower R^2 for C/N ratio in some heaps reflects the additional complexity of nitrogen cycle processes, including ammonia volatilisation, nitrification, and microbial nitrogen immobilisation, which introduce non-linearities not captured by the first-order model (Tiquia et al. 1996).

The range of TOC rate constants (0.0135 to 0.0192 day^{-1}) and VOC rate constants (0.0105 to 0.0211 day^{-1}) observed in this study bracket values reported in the broader biopolymer composting literature. Nair et al. (2016) similarly reported that PLA composting under windrow conditions is well described by first-order carbon decline kinetics, and comparable rate constants have been reported for other biopolymer composting systems (Ruggero et al. 2022), supporting the robustness of the first-order model as applied here.

Moisture attenuation is likewise not a biodegradation process; it results from the combined action of evaporation, turning-induced aeration and metabolic heat generation. The first-order coefficient reported for moisture is accordingly an empirical attenuation coefficient rather than a degradation rate. Its approximately log-linear behaviour arises because the dominant driver, evaporative loss, is proportional to the metabolic heat released during substrate oxidation, which itself declines first-order, so that moisture loss is paced by and coupled to the carbon mineralisation (Haug 1993). The strong goodness-of-fit obtained for moisture, in contrast to the C/N ratio, reflects the fact that evaporative drying is a smoothly decaying physical process; the attenuation coefficient is therefore useful for predicting the duration of the active phase and the onset of maturation rather than for quantifying biodegradation.

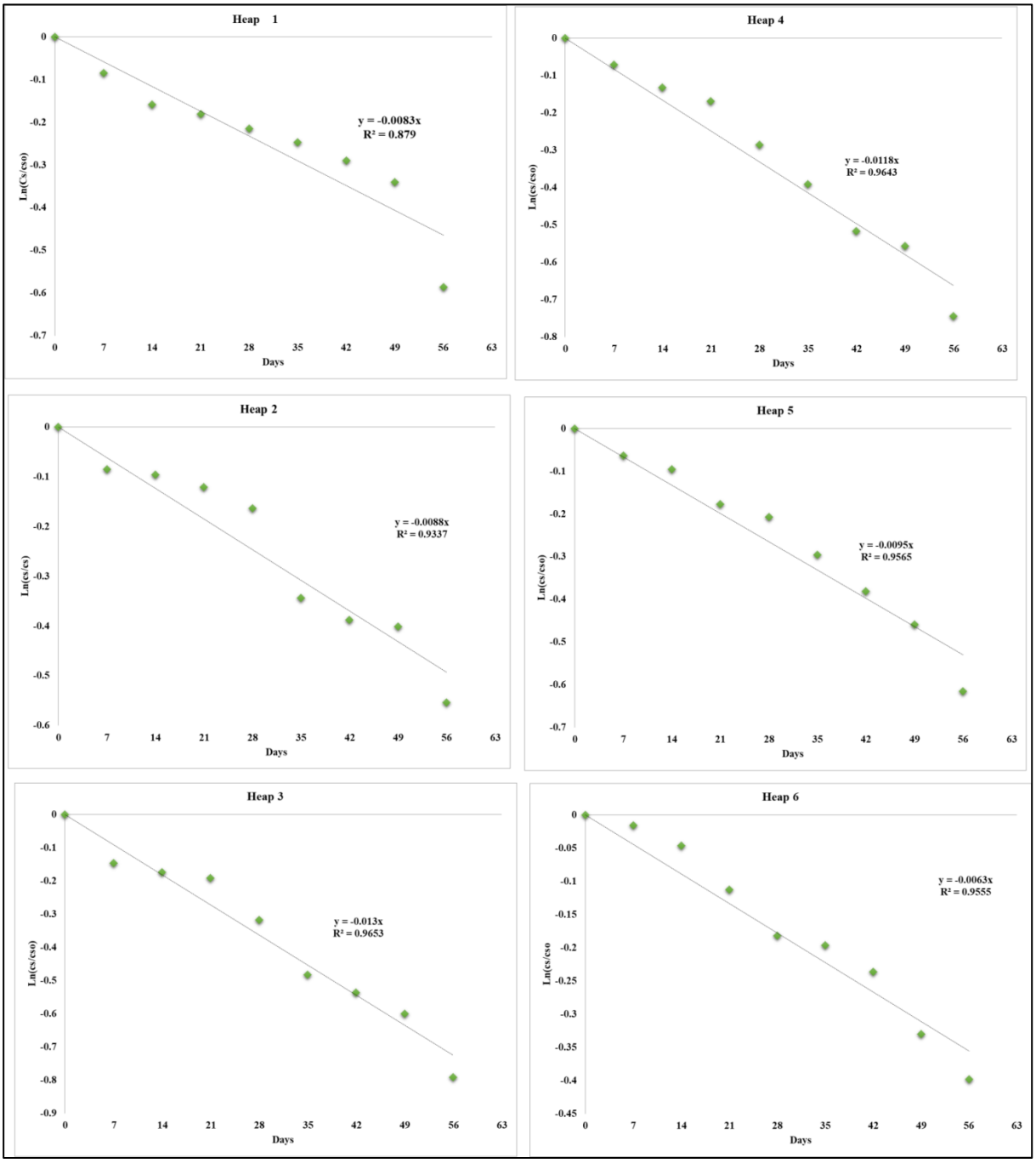

Figure 4: ln(Moisture / Moisture$_0$) versus composting time for Heaps 1 to 6. Heap 5 anomalous k value should be noted in the figure legend. X-axis: Time (days); Y-axis: ln(Cs/C$_0$). Solid regression lines with R² annotations.

Table 5. Consolidated first-order rate constants (k, day^{-1}) and coefficients of determination (R^2) for all parameter-heap combinations.

Heap	TOC		VOC		C/N Ratio		Moisture Content	
	k (day^{-1})	R^2	k (day^{-1})	R^2	k (day^{-1})	R^2	k (day^{-1})	R^2
Heap 1	0.0151	0.967	0.0211	0.991	0.0103	0.835	0.0083	0.962
Heap 2	0.0155	0.963	0.0175	0.991	0.0119	0.092	0.0088	0.977
Heap 3	0.0192	0.984	0.0136	0.961	0.0129	0.962	0.0130	0.989
Heap 4	0.0184	0.992	0.0117	0.913	0.0092	0.807	0.0118	0.989
Heap 5	0.0135	0.991	0.0137	0.958	0.0101	0.839	0.0995*	0.985
Heap 6	0.0143	0.972	0.0105	0.979	0.0096	0.891	0.0063	0.983

3.6 Spectroscopic and Morphological Evidence of PLA Degradation

Scanning electron microscopy coupled with energy-dispersive X-ray spectroscopy (SEM–EDS; JEOL JSM-IT 200, 20.0 kV) was used to obtain direct morphological evidence of PLA surface transformation. At Day 0, the PLA particles presented smooth, featureless planar surfaces with well-defined angular geometry, sharp edges and minimal porosity, and particle sizes of 50–300 µm, confirming that no degradation had been initiated in the freshly assembled heaps. By Day 56, all PLA-amended heaps exhibited pronounced surface deterioration that intensified with PLA loading. At the lower loading, surfaces showed pitting, shallow crack formation and partial fragmentation, with particle sizes reduced to 20–150 µm. At the intermediate loading, extensive surface roughening, interconnected pore networks, crack propagation, surface-layer peeling and 10–100 µm fragments were observed. At the highest loading, the most severe breakdown occurred, comprising extensive surface erosion, high macroporosity, loss of coherent filmy morphology, brittle fracture surfaces and fragmentation into fine irregular particles of less than 10–50 µm. This progression from intact to defect-rich, eroded morphology is the characteristic signature of surface-erosion-driven polyester biodegradation, in which esterase-mediated hydrolysis preferentially attacks the accessible amorphous domains before the semi-crystalline regions (Tokiwa and Calabia 2006; Husárová et al. 2014; Hajilou et al. 2024). An equivalent evolution from smooth surfaces to cracked and voided surfaces has been reported for PLA degraded under controlled composting conditions (Luo et al. 2019).

FTIR spectroscopy (PerkinElmer Spectrum Two, 4000–400 cm^{-1}) of the Day 56 compost confirmed the molecular presence of PLA and the state of its ester-bond environment. The methyl ester CH_3 deformation of PLA was retained at 1416 cm^{-1}, and the PLA ester C–O–C stretch was resolved in the 1040–1080 cm^{-1} region, the transmittance of which varied systematically with PLA loading in a manner consistent with an ester population undergoing progressive hydrolytic loss. A broad O–H/N–H

stretching envelope at 3302 cm^{-1} and amide I / aromatic C=C features near 1625 cm^{-1} reflected hydroxyl groups, including the hydroxyl and carboxyl chain ends generated by ester-bond scission, together with the protein-derived and humic structures formed during maturation. The mildly alkaline terminal pH of the heaps (8.31–8.53) further favours base-catalysed hydrolysis of the PLA ester linkage ($R–CO–O–R' + OH^- \rightarrow R–COO^- + HO–R'$), which complements enzymatic depolymerisation during the cooling and maturation phase (Tokiwa and Calabia 2006; Momeni et al. 2023). The random scission of ester bonds in the amorphous regions, with the attendant release of carboxyl-terminated oligomers and lactic acid, is the accepted primary route of PLA degradation in compost and is consistent with the spectroscopic and morphological changes observed here, though molecular-weight analysis was not performed to directly confirm chain scission. (Momeni et al. 2023; Hajilou et al. 2024).

The present study did not assess the mass loss of PLA, the percentage of disintegration, the evolved CO_2, or the reduction in molecular weight using gel-permeation chromatography. Furthermore, differential scanning calorimetry was not performed. The evidence for PLA degradation reported here is therefore based on direct molecular (FTIR) and morphological (SEM–EDS) observations rather than on gravimetric or respirometric mineralisation metrics. These complementary observations are nevertheless recognised, polymer-specific indicators of PLA breakdown (Luo et al. 2019; Momeni et al. 2023; Hajilou et al. 2024) and are consistent with the bulk-parameter kinetics reported in Sections 3.2–3.5. Quantitative mass-loss, respirometric CO_2 and GPC molecular-weight determinations are identified as priorities for subsequent work to establish a complete mineralisation mass balance.

3.7 Compost Maturity and Stability Assessment

Compost maturity was evaluated against multiple independent indicators rather than the C/N ratio and TOC reduction alone. By Day 56 all heaps satisfied the principal maturity criterion, with terminal C/N ratios of 10.41–11.39 lying below the maturity threshold of 15 and approaching the 10–12 range associated with advanced stabilisation (Bernal et al. 2009), alongside TOC reductions of 50.9–71.6%. These were corroborated by three further measured indicators. First, pH rose from an initially acidic-to-neutral 6.51–6.82 to a mildly alkaline 8.31–8.53, within the 7.5–8.5 range recommended for mature, agronomically safe compost (European Commission 2001), reflecting completed ammonification and organic-acid depletion. Second, electrical conductivity increased from 1.02–1.18 to 1.55–1.89 mS cm^{-1}, remaining well below the 4.0 mS cm^{-1} phytotoxicity threshold and indicating that no treatment produced saline compost liable to impair seed germination or root elongation. Third, heap temperatures returned to within one to two degrees of ambient (30.2–31.5 °C) by Day 56, confirming the cessation of active exothermic decomposition and thermal stabilisation. Terminal total Kjeldahl nitrogen of 1.65–1.99% additionally fell within the 1.5–2.5% benchmark for mature composts (Bernal et al. 2009). The convergence of these independent chemical, ionic and thermal indicators provide substantially stronger evidence of stabilisation than the C/N ratio and TOC reduction alone.

It is nevertheless recognised that biological maturity was not assessed directly in this study. Seed-germination-index and root-elongation phytotoxicity bioassays, microbial respiration or oxygen-uptake

rate, and ecotoxicity testing were outside the scope of the present physicochemical investigation. Because these biological assays provide the definitive confirmation of a phytotoxicity-free, biologically stable product, and because residual lactic acid oligomers released during PLA hydrolysis could in principle exert transient phytotoxicity, they are identified as priority future work. The maturity of the compost is therefore reported here as advanced physicochemical stabilisation, pending biological confirmation.

Table 6. Compost maturity and stability indicators at Day 56 (Set I, Heaps 1–6).

Indicator	Day 56 value	Maturity / safety benchmark	Status
C/N ratio	10.41–11.39	< 15 mature; 10–12 advanced	Met (advanced)
TOC reduction	50.9–71.6%	> 50%	Met
pH	8.31–8.53	7.5–8.5 (EC 2001)	Met
Electrical conductivity	1.55–1.89 mS cm^{-1}	< 4.0 mS cm^{-1}	Met
Temperature stabilisation	30.2–31.5 °C	return to near-ambient	Met
Total Kjeldahl nitrogen	1.65–1.99%	1.5–2.5% (mature)	Met

3.8 Inter-Heap Variability and Process Implications

The range of k values across heaps shows how unique conditions affect PLA degradation rates. For TOC, the highest-to-lowest k ratio is 1.42 (Heap 3 compared to Heap 5) indicating heap composition can cause a 42% change in carbon breakdown rate. In practice, with k = 0.0192 day^{-1}, it takes about 36.1 days to reduce TOC by 50% (half-life, $t_{½} = \ln 2/k$). However, with k = 0.0135 day^{-1}, the half-life increases to 51.3 days, which is more than two weeks longer in the same setup. These differences impact how composting facilities are designed for waste contaminated with PLA. Process engineers need to think about how the feedstock's kinetic variability affects compost pad retention times, windrow management schedules, and certification compliance timelines. The first-order kinetic framework used here helps pilot-scale rate constants guide full-scale predictions and optimize conditions within the timeframes of regulatory compost quality standards. (Bernal et al. 2009; Hottle et al., 2017).

4. Conclusions

This study examined how PLA-based biopolymer solid waste breaks down in six compost heaps. The PLA content ranged from 0 to 50% and was mixed with vegetable waste and cow dung over 56 days. The study employed a first-order kinetic analysis to examine four bulk process parameters, in conjunction with direct spectroscopic and morphological assessments of the polymer. The bulk carbon parameters followed to first-order kinetics under the experimental conditions. The degradation rate constants for total organic carbon (TOC) varied between 0.0135 and 0.0192 day^{-1}, whereas volatile organic compounds (VOC) exhibited rate constants ranging from 0.0105 to 0.0211 day^{-1}. These constants characterize the mineralization of the entire composting matrix that offers a validated

and uncertainty-bounded basis for process design and prediction. The C/N ratio and moisture content showed first-order trends. However, they are described using empirical stabilization and attenuation coefficients instead of direct biodegradation rates. Moisture loss occurs due to evaporation caused by metabolic heat. The recalculation process revealed that the previously anomalous values for the C/N ratio of Heap 2 and the moisture content of Heap 5 were due to transcription errors, which have now been corrected. The C/N ratio exhibited the broadest confidence intervals due to its nature as a derived ratio. To establish polymer-specific evidence, FTIR and SEM–EDS analyses verified the structural degradation of the PLA fraction. By Day 56, the polymer particles transitioned from smooth, intact surfaces to heavily pitted, cracked, and fragmented residues. The FTIR spectra revealed a decrease in the PLA ester bands and the emergence of hydroxyl groups, signifying ester-bond hydrolysis. This degradation occurred under genuinely thermophilic conditions, with peak temperatures ranging from 53 to 59 °C, surpassing the PLA glass-transition threshold. Consequently, this facilitated the hydrolytic chain scission initiating polymer breakdown. The study demonstrates that PLA degradation occurred most intensely at a PLA loading of 20 to 30%, corresponding with the highest bulk carbon-degradation rate constants. However, the first-order rate constants presented here pertain to bulk compost parameters under the tested conditions and do not specifically represent PLA mineralisation kinetics. The bulk measurements encompass PLA, vegetable waste, cow dung, and inoculum fractions, and since quantitative PLA-specific metrics (such as mass loss, disintegration percentage, evolved CO_2, and molecular-weight reduction) were not assessed, the precise rate of PLA mineralisation remains undetermined. The attribution of degradation to the PLA fraction is supported by convergent evidence from polymer-specific FTIR and SEM changes, dose-dependent trends across the 0 to 50% PLA series compared to the PLA-free control, and the thermophilic temperature regime, rather than a direct carbon mass balance.

By Day 56 the compost had attained advanced physicochemical stabilisation, indicated by the convergence of terminal C/N ratios (10.41 to 11.39), TOC reductions (50.9 to 71.6%), a mildly alkaline pH (8.31 to 8.53), electrical conductivity below the 4.0 mS cm^{-1} phytotoxicity threshold (1.55 to 1.89 mS cm^{-1}) and near-ambient final temperatures. Biological maturity indicators, namely the germination index, respiration rate and phytotoxicity bioassay, were not measured and are required to confirm full biological maturity. Within these bounds, the study provides quantitative, uncertainty-bounded first-order benchmarks for the bulk composting behaviour of PLA-amended windrows, together with direct evidence that PLA structural degradation proceeds under thermophilic composting, of relevance to industrial biopolymer waste management and compost-quality certification. Future work should establish PLA-specific mineralisation kinetics through gravimetric mass-loss, respirometric CO_2 evolution and gel-permeation-chromatography molecular-weight measurements, referenced against PLA-free and sterilised abiotic controls, and should incorporate biological maturity and phytotoxicity assays to complete the end-of-life assessment.

5. Acknowledgment

The authors express sincere gratitude to the Annamalai University, Department of Civil Engineering, for providing necessary laboratory facility and other infrastructure for carrying out this research work. The authors further wish to acknowledge and thank the Ministry of Human Resource Development (MHRD) for extending the financial support under RUSA 2.0 research grant for this study.

6. Funding Declaration

The authors further wish to acknowledge and thank the Ministry of Human Resource Development (MHRD) for extending the financial support under RUSA 2.0 research grant for this study.

7. References

Agnew, J.M. and Leonard, J.J., 2003. The physical properties of compost. Compost Science and Utilization, 11(3), pp. 238–264.

APHA, 2017. Standard Methods for the Examination of Water and Wastewater. 23rd ed. Washington, DC: American Public Health Association.

ASTM, 2019. ASTM D6400-19: Standard Specification for Labeling of Plastics Designed to be Aerobically Composted in Municipal or Industrial Facilities. West Conshohocken, PA: ASTM International.

Bagheri, A.R., Laforsch, C., Greiner, A. and Agarwal, S., 2017. Fate of so-called biodegradable polymers in seawater and freshwater. Global Challenges, 1(4), 1700048.

Bernal, M.P., Alburquerque, J.A. and Moral, R., 2009. Composting of animal manures and chemical criteria for compost maturity assessment: a review. Bioresource Technology, 100(22), pp. 5444–5453.

CEN, 2000. EN 13432:2000 – Packaging: Requirements for Packaging Recoverable Through Composting and Biodegradation. Brussels: European Committee for Standardization.

De Jong, S.J., Arias, E.R., Rijkers, D.T.S., van Nostrum, C.F., Kettenes-van den Bosch, J.J. and Hennink, W.E., 2001. New insights into the hydrolytic degradation of poly(lactic acid): participation of the alcohol terminus. Polymer, 42(7), pp. 2795–2802.

European Bioplastics, 2023. Bioplastics Market Data 2023. Berlin: European Bioplastics Association.

European Commission, 2001. Working Document: Biological Treatment of Biowaste (2nd draft). Brussels: European Commission, Directorate-General Environment.

Garlotta, D., 2001. A literature review of poly(lactic acid). Journal of Polymers and the Environment, 9(2), pp. 63–84.

Geyer, R., Jambeck, J.R. and Law, K.L., 2017. Production, use, and fate of all plastics ever made. Science Advances, 3(7), e1700782.

Hajilou, N., Mostafayi, S.S., Yarin, A.L. and Shokuhfar, T., 2024. A comparative review on biodegradation of poly(lactic acid) in soil, compost, water, and wastewater environments: incorporating mathematical modeling perspectives. AppliedChem, 5(1), 1.

Hamelers, H.V.M., 2004. Modeling composting kinetics: a review of approaches. Reviews in Environmental Science and Bio/Technology, 3(4), pp. 331–342.

Haug, R.T., 1993. The Practical Handbook of Compost Engineering. Boca Raton, FL: Lewis Publishers.

Hottle, T.A., Bilec, M.M. and Landis, A.E., 2017. Biopolymer production and end-of-life comparisons using life cycle assessment. Resources, Conservation and Recycling, 122, pp. 295–306.

Husárová, L., Pekřová, S., Stloukal, P., Kucharczyk, P., Verney, V., Commereuc, S., Ramone, A. and Koutýný, M., 2014. Identification of important abiotic and biotic factors in the biodegradation of poly(lactic acid). International Journal of Biological Macromolecules, 71, pp. 155–162.

ISO 11465, 1993. Soil Quality: Determination of Dry Matter and Water Content on a Mass Basis. Geneva: International Organization for Standardization.

Jem, K.J. and Tan, B., 2020. The development and challenges of poly(lactic acid) and poly(glycolic acid). Advanced Industrial and Engineering Polymer Research, 3(2), pp. 60–70.

Kale, G., Kijchavengkul, T., Auras, R., Rubino, M., Selke, S.E. and Singh, S.P., 2007. Compostability of bioplastic packaging materials: an overview. Macromolecular Bioscience, 7(3), pp. 255–277.

Komilis, D.P. and Ham, R.K., 2006. Carbon dioxide and ammonia emissions during composting of mixed paper, yard waste and food waste. Waste Management, 26(1), pp. 62–70.

Laycock, B., Nikolić, M., Colwell, J.M., Gauthier, E., Halley, P., Bottle, S. and George, G., 2017. Lifetime prediction of biodegradable polymers. Progress in Polymer Science, 71, pp. 144–189.

Lazcano, C., Gomez-Brandon, M. and Dominguez, J., 2008. Comparison of the effectiveness of composting and vermicomposting for the biological stabilization of cattle manure. Chemosphere, 72(7), pp. 1013–1019.

Luo, Y., Lin, Z. and Guo, G., 2019. Biodegradation assessment of poly(lactic acid) filled with functionalized titania nanoparticles (PLA/TiO_2) under compost conditions. Nanoscale Research Letters, 14, 56.

Manna, L., Zanetti, M.C. and Genon, G., 2017. Modelling and preliminary design of composting process. Journal of Loss Prevention in the Process Industries, 49, pp. 392–401.

Momeni, S., Craplewe, K., Safder, M., Luz, S., Sauvageau, D. and Elias, A., 2023. Accelerating the biodegradation of poly(lactic acid) through the inclusion of plant fibers: a review of recent advances. ACS Sustainable Chemistry and Engineering, 11(41), pp. 14539–14563.

Nair, N.R., Sekhar, V.C., Nampoothiri, K.M. and Pandey, A., 2016. Biodegradation of biopolymers. In: A. Pandey, S. Negi and C.R. Soccol (eds.) Current Developments in Biotechnology and Bioengineering: Production, Isolation and Purification of Industrial Products. Amsterdam: Elsevier, pp. 739–755.

Ncube, L.K., Ude, A.U., Ogunmuyiwa, E.N., Zulkifli, R. and Beas, I.N., 2021. An overview of plastic waste generation and management in food packaging industries. Recycling, 6(1), p. 12.

Nelson, D.W. and Sommers, L.E., 1982. Total carbon, organic carbon, and organic matter. In: A.L. Page (ed.) Methods of Soil Analysis, Part 2, 2nd ed. Madison, WI: American Society of Agronomy, pp. 539–579.

Piemonte, V., Sabatini, S. and Gironi, F., 2013. Chemical recycling of PLA: a great opportunity towards sustainable development? Journal of Polymers and the Environment, 21(3), pp. 640–647.

Rhim, J.W., Park, H.M. and Ha, C.S., 2013. Bio-nanocomposites for food packaging applications. Progress in Polymer Science, 38(10–11), pp. 1629–1652.

Rudnik, E. and Briassoulis, D., 2011. Degradation behaviour of poly(lactic acid) films and fibres in soil under Mediterranean field conditions and laboratory simulations testing. Industrial Crops and Products, 33(3), pp. 648–658.

Ruggero, F., Belardi, S., Carretti, E., Lotti, T., Lubello, C. and Gori, R., 2022. Rigid and film bioplastics degradation under suboptimal composting conditions: a kinetic study. Waste Management & Research, 40. https://doi.org/10.1177/0734242X211063731

Rujnic-Sokele, M. and Pilipovic, A., 2017. Challenges and opportunities of biodegradable plastics: a mini review. Waste Management and Research, 35(2), pp. 132–140.

Tiquia, S.M., Tam, N.F.Y. and Hodgkiss, I.J., 1996. Microbial activities during composting of spent pig-manure sawdust litter at different moisture contents. Bioresource Technology, 55(3), pp. 201–206.

Tokiwa, Y. and Calabia, B.P., 2006. Biodegradability and biodegradation of poly(lactide). Applied Microbiology and Biotechnology, 72(2), pp. 244–251.

Tsuji, H., 2010. Poly(lactic acid). In: R. Auras, L.T. Lim, S.E.M. Selke and H. Tsuji (eds.) Poly(lactic acid): Synthesis, Structures, Properties, Processing, and Applications. Hoboken, NJ: Wiley, pp. 107–131.

Walkley, A. and Black, I.A., 1934. An examination of the Degtjareff method for determining soil organic matter, and a proposed modification of the chromic acid titration method. Soil Science, 37(1), pp. 29–38.